Formations of narrow stripes and vortex-antivortex pairs in a quasi-two-dimensional ferromagnet K_2CuF_4

Yoshihiko Togawa[1], Tetsuya Akashi[2], Hiroto Kasai[2], Gary W. Paterson[3], Stephen McVitie[3], Yusuke Kousaka[1], Hiroyuki Shinada[2], Jun-ichiro Kishine[4], and Jun Akimitsu[5]

[1]*Department of Physics and Electronics, Osaka Prefecture University, 1-1 Gakuencho, Sakai, Osaka 599-8531, Japan*
[2]*Research and Development Group, Hitachi Ltd., Hatoyama 350-0395, Japan*
[3]*SUPA, School of Physics and Astronomy, University of Glasgow, Glasgow G12 8QQ, United Kingdom*
[4]*Division of Natural and Environmental Sciences, The Open University of Japan, Chiba 261-8586, Japan*
[5]*Research Institute for Interdisciplinary Science, Okayama University, Okayama 700-8530, Japan*

Using cryogenic Lorentz transmission electron microscopy, we investigate the temperature evolution of magnetic structures in single crystal samples of K_2CuF_4 with a magnetic phase transition at 6.1 K. This material is known as one of the candidates for a two-dimensional (2D) *XY* magnet that may exhibit a Berezinskii-Kosterlitz-Thouless (BKT) phase transition. A fine magnetic stripe pattern was found with a period of about 120 nm in a direction along the *c* axis below 7.3 K in a thin sample with the *c* axis in the plane. Magnetic columns of vortices and antivortices with a separation of about three micrometers were observed below 6 K in a *c*-plane sample approximately 150 nm in thickness. The formation of two different types of magnetic structures at different threshold temperatures is likely to be consistent with a picture of two-step dimensional crossover in spin and real spaces previously derived from magnetization and neutron experiments in K_2CuF_4. These results indicate how the 2D *XY* character of K_2CuF_4 is incorporated in three-dimensional magnetic structures. Based on the experimental observations, we discuss the lengthscale of film thickness appropriate for expanding the 2D *XY* regime and generating the robust BKT excitations. We expect our study to be an important step in realizing the BKT phase transition in a real magnetic system.

KEYWORDS: Lorentz microscopy, K_2CuF_4, narrow stripe, vortex and antivortex pair, two-dimensional *XY* magnet, Berezinskii-Kosterlitz-Thouless phase transition

Introduction. — The dimensionality of a system has a strong influence on its structure and dynamics. Indeed, the nature of the phase transition in a low-dimensional system has attracted considerable interest for many decades. One of the celebrated works in the field is the proposal of the topological ground state in the two-dimensional (2D) spin system, which was made by Kosterlitz and Thouless[1–3] and awarded the Nobel Prize in Physics 2016.[4]

Prior to these proposals, many significant advances were made in understanding the phase transition in the low-dimensional system. Stanley and Kaplan found that a divergence of susceptibility may occur at a finite temperature as an indication of the phase transition in the 2D system of Heisenberg spins.[5] Additionally, Mermin and Wagner explicitly demonstrated that ordering of Heisenberg and *XY* spins is prevented by thermal fluctuations in one and two dimensions.[6] Namely, no ordered phase and no spontaneous magnetization appear at a finite temperature.

This paradoxical situation was resolved by Kosterlitz and Thouless.[1–3] They derived that the phase transition occurs at a finite temperature given by πJ (T_{KT}) where quasi long-range order emerges in the 2D system of *XY* spins through the formation and unbinding of vortex-antivortex pairs. Here, J is the exchange interaction of the system. Berezinskii independently pointed out the importance of vortex excitations in the *XY* model.[7,8] In summary, the 2D *XY* model enables magnetic vortex and antivortex excitations and undergoes a phase transition of vortex and antivortex unbinding, referred to as BKT phase transition.[9]

The existence of the BKT phase transition was experimentally demonstrated in a thin 2D film of Helium[10] as well as in a superconducting Josephson network.[11] However, to our surprise, no reliable experimental demonstration of the BKT phase transition has been performed in a magnetic system.[9] This is mainly due to the following two reasons: 1) 2D *XY* magnets appropriate for the BKT phase transition were not readily available. 2) The techniques commonly used in the study of these materials were not capable of directly observing the BKT phenomena.

In this study, we focus a quasi-2D ferromagnet K_2CuF_4, which is one of the promising candidates that may exhibit the BKT phase transition, as first proposed nearly 40 years ago[12] by Hirakawa. This material is known to exhibit a cascade of dimensional crossover in spin and real spaces: with reducing temperature, the magnetic crossover occurs at around 7.3 K (T^*) in spin space from 2D Heisenberg to 2D *XY*, followed by the one into 3D *XY* in real space below the ferromagnetic phase transition temperature T_{C} of 6.25 K.[12] These features of the dimensional crossover in K_2CuF_4 are presented in table I(a). Cryogenic Lorentz transmission electron microscopy (TEM) is employed in order to directly observe the formation of magnetic structures upon the magnetic phase transitions in two kinds of thin lamellae of the K_2CuF_4 single crystal.

First, we examined magnetic structures in a 100 nm thick TEM sample, where the *c* axis orients within the sample plane. In this case, we do not expect that vortices are accommodable within the *c* plane because of the sample geometry. Instead, a magnetic stripe pattern with a period of about 120 nm was found along the *c* axis at zero magnetic field below 7.3 K. This temperature is apparently higher than T_{C} and coincides with the crossover temperature T^* below which the 2D *XY* nature becomes relevant.

We also studied the formation of magnetic structures in a different TEM sample, made of the *c*-plane film with an electron transparent (150 nm thick) area of 7 μm × 5 μm. This observation area was supported by thick parts of the crystal from two opposing sides. We directly saw that magnetic columns of vortices and antivortices emerged and were frozen below a temperature of 6 K, namely in the 3D *XY* regime. Only two sets of vortex and antivortex pancakes are accommodated and stack pairwise over the *c*-plane layers because of the confined geometry of the sample. The vortices survive up to 50 Oe when vertical magnetic fields are applied in a direction nearly normal to the *c* plane of the sample. With further increasing the strength of magnetic fields, the sample displayed a uniformly magnetized state within the plane. The formation of such 3D magnetic structures with the in-plane magnetic components being dominant is consistent with an enhancement of the *XY* character at low temperatures due to hard-axis crystalline anisotropy as well as a development of interlayer correlation via the interlayer exchange coupling reported in K_2CuF_4.[12)]

Therefore, our experimental observations of narrow stripes as well as vortices and antivortices at different threshold temperatures are consistent with a picture of two-step dimensional crossover of K_2CuF_4 including the presence of the 2D *XY* regime.

Magnetic characteristics. — K_2CuF_4 is a typical quasi-2D ferromagnetic material with $S = 1/2$ and T_C of 6.25 K.[13)] The experimentally derived material parameters of this compound are as follows. The tetragonal unit cell has a lattice constant of 0.413 nm in the *a* axis and 1.267 nm in the *c* axis. The intralayer isotropic exchange interaction J (within the *c* plane) is as large as 11.4 K,[14)] while the interlayer exchange J' (along the *c* axis) is 0.0088 K.[15)] That J' is three orders of the magnitude smaller than J makes this spin system almost decoupled among layers. The Ising nature within the plane is negligibly small. The hard-axis crystalline anisotropy J_A is 0.11 K,[16)] which is a hundred times smaller than J. Therefore, the spin symmetry of K_2CuF_4 is of almost 3D Heisenberg type with 1 % *XY* characteristics.

Note that, as the temperature reduces toward T_C, the 2D *XY* nature of the spin system becomes significant in the magnetically anisotropic material.[17,18)] Indeed, at low temperature, where the spin correlation length ξ extends over a characteristic lengthscale given by $a\sqrt{J/J_A}$ with a being a lattice constant, K_2CuF_4 behaves like a good 2D *XY* spin system.[12)]

In order to clarify the 2D *XY* nature of K_2CuF_4, the magnetic properties were intensively examined around T_C by means of neutron scattering[19–24)] and magnetization measurements[25–28)] in 1970s and early 1980s. In particular, critical exponents were determined by static magnetization and neutron scattering measurements.[12)] The critical indices determined in the 2D *XY*-like crossover regime were in good agreement with the Kosterlitz theory and the Monte Carlo simulation.[29,30)] The crossover temperature T^* from 2D Heisenberg (at high temperatures) to 2D *XY* was determined to be 7.3 K, below which ξ becomes larger than $a\sqrt{J/J_A}$ as reported in the neutron scattering data. Importantly, the other crossover temperature between 2D *XY* and 3D *XY*, where ξ exceeds $a\sqrt{J/J'}$, was consistent with the value of T_C. These magnetic characteristics of K_2CuF_4 are briefly summarized in Table I(a). For reference, the typical behavior of the BKT transition expected for a 2D *XY* system with no interlayer exchange (J'=0) is also shown in Table I(b). Here, T_{KT} corresponds to the BKT phase transition temperature.

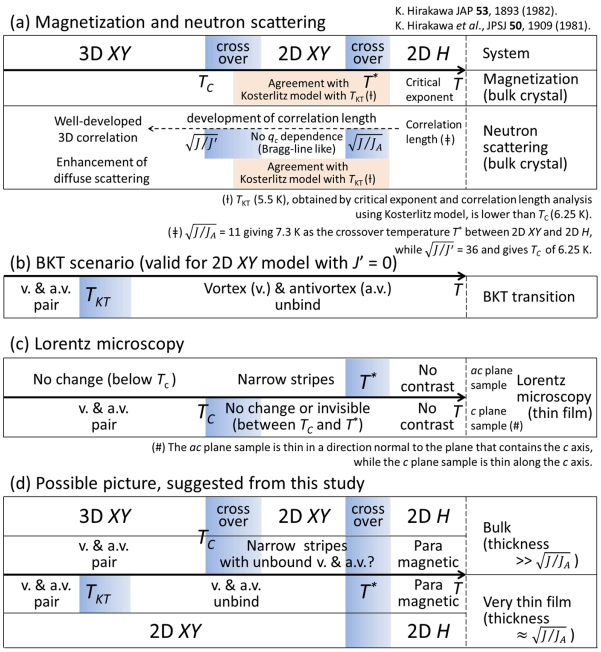

Table I. A brief summary of magnetic characteristics of a K_2CuF_4 single crystal. The horizontal direction corresponds to temperature. (a) Two-step dimensional crossover in spin and real space was observed in magnetization and neutron scattering experiments performed by Hirakawa *et al*. (For example, see Refs. 12 and 28.) In their studies, T_{KT} was determined to be 5.5 K based on critical exponent and correlation length analysis using Kosterlitz model. T_C was 6.25 K in the magnetization measurements, which was consistent with the value obtained by the correlation length analysis with a criterion that $\sqrt{J/J'} = 36$. The crossover temperature T^* between 2D *XY* and 2D Heisenberg (2D *H*) was determined as 7.3 K, at which temperature the correlation length exceeded $\sqrt{J/J_A}$ (= 11). Note that large intensity of the diffuse scattering was observed in the 3D *XY* regime below T_C in the neutron experiments, the origin of which remains unclear. (b) Typical behavior of the BKT transition expected for the 2D *XY* system with $J' = 0$. A vortex is represented by 'v', and antivortex by 'a.v.' (c) The results obtained by cryogenic Lorentz microscopy in this study. The *ac* plane sample is thin in a direction normal to the plane that contains the *c* axis, while the *c* plane sample is thin along the *c* axis. (d) A possible picture of the development of the magnetic structures in bulk crystals and very thin films, which is proposed based on the results obtained in this study as well as the previously obtained knowledge on K_2CuF_4 crystals.

Furthermore, the diffuse scattering was found to occur below T_C in the 3D *XY* regime in addition to the conventional magnetic Bragg scattering in K_2CuF_4.[19)] This means that giant transverse susceptibility develops even below T_C. The authors in Refs. 19 and 31 argued the origin of this anomalous behavior in terms of weak correlations among the layers and pointed out the possible existence of 1D-like (c-axis oriented) solitons formed out of the strongly correlated intralayer spins.[31)] They also discussed the possibility of the formation of paired vortices at low density within the layer, which may be a symptom of the BKT phase transition. In this connection, they examined the temperature dependence of the diffuse scattering intensity in the 3D *XY* regime and found a sudden reduction of the intensity at T_C.[12)] They argued that this data might indicate the change of the exchange stiffness J at T_C (not at T_{KT}) and be regarded as a symptom of the universal jump which occurred in a modified form. However,

their interpretation has not been verified directly, for example, by experimental imaging of the magnetic structure around the phase transition.

In terms of direct observation of magnetic structures, previous studies by magneto-optical imaging via Faraday rotation using visible light of 546 nm has been performed below T_C in this transparent compound.[32,33] Magnetic stripe domains with a typical width of 4 μm were observed in the direction parallel to the *c* plane (perpendicular to the *c* axis) in the *ac*-plane sample. No observation was performed in the *c*-plane sample. Unfortunately, the lack of spatial resolution hampers detailing the nature and origin of the observations from neutron scattering experiments[19,31], which infer the formation of locally ordered regions with giant magnetic moments accompanying vortex structures (recognized as 'condensed magnons') in the *c* plane below T_C. Therefore, direct observation of vortices formation at higher spatial resolution has been eagerly desired in this fascinating spin system.

Sample preparation. — A transparent bulk single crystal of K_2CuF_4 was used in this study. The crystal quality including its orientation was examined based on Laue diffraction patterns and the magnetization data taken using SQUID magnetometry. The T_C of the bulk crystal was evaluated to be 6.1 K, which is consistent with values reported in the literature.[12] For TEM observations, thin platelet samples with different crystal orientations with windows of uniform thickness were fabricated from the bulk single crystal using a focused ion beam (FIB) method. Two kinds of TEM samples were prepared to see anisotropic behavior of the magnetization: one has the *c* axis orienting within the plane, while the other is the *c*-plane lamella. The TEM samples were confirmed to be of single crystal by using TEM images and electron diffraction data. As for the sample geometry, areas transparent to electron beam were supported by thick parts of the crystal from two opposing sides in order to ensure good thermal conductance.

Experimental method. — Lorentz TEM observations were performed using a field-emission electron microscope with an acceleration voltage of 1 MV (Hitachi H-1000FT).[34] This machine has many advantages in observing magnetic structures using a coherent electron beam with a wavelength of 0.87 pm.[35] In particular, it is equipped with a dedicated system for the magnetic field application using superconducting magnets,[36] which is located above the objective lens. In this position, the residual magnetic field generated by the electromagnetic lenses including the objective lens is as small as the strength of Earth's magnetic field (< 0.45 G). A TEM sample, being mounted on a liquid Helium holder and installed into the system, is subject to configurable magnetic fields from the surrounding superconducting magnets in all three dimensions.[37] When the sample and magnets are cooled with liquid Helium, thermal radiation is significantly suppressed compared to that in a conventional experimental setup which uses a liquid Helium holder in a commercial TEM machine. In the present case, the sample can be cooled down to 4.3 K stably. A deviation of the temperature between the sample and thermometer located beside it was found to be less than 0.1 K in a separate TEM experiment to measure the T_C of the small bulk crystal with a hole[38] which has almost the same dimensions as the TEM samples except for the thickness. This experiment also indicated that the TEM samples are supposed to have the same value of T_C as the original bulk crystal since these samples were fabricated with the same procedure using a FIB method.

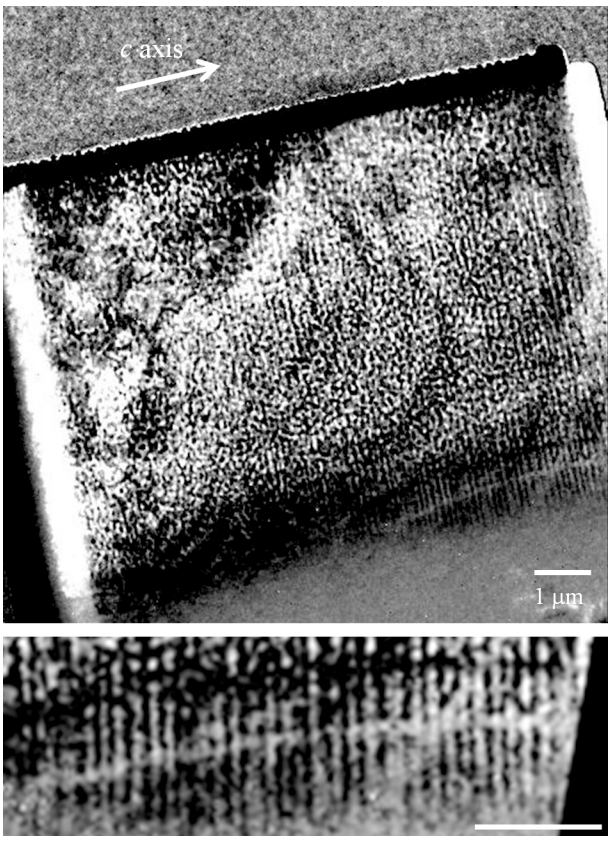

Fig. 1. Lorentz image of the TEM sample with the *c* axis orienting within the plane at zero magnetic field at 5.2 K. The sample size is 10 μm (along *c* axis) × 8 μm × 0.1 μm. The scale bar corresponds to the length of 1 μm.

Lorentz micrographs of the magnetic structures in K_2CuF_4 were taken at a fixed strength of the applied magnetic field at temperatures around T_C in the Fresnel mode of Lorentz microscopy.[39] A temperature dependence of the sample magnetization was monitored with a K2 camera by recording a movie with a rate of one frame/s while the temperature was swept between 5.0 K and 8.5 K at 0.02 K/s. In this respect, the present method is sensitive only to almost static magnetic structures, with any faster dynamics being recorded as an average.

To analyze the magnetic structure, a sample drift due to the temperature change was corrected across frames of the original movie and a series of differential Lorentz images were made from the neighboring frames. The contrast in the defocused images is expected to show the magnetic structure and in particular the differential Lorentz images should reveal a change in the magnetic structure. Furthermore, a similar technique used in the projection electron-beam magnetic tomography analysis[40,41] was adopted for a visualization of the magnetic structure, where the magnetic field can be quantified by analyzing distortions of TEM images.

Lorentz micrographs. — Figure 1 shows the Lorentz image of a different TEM sample that contains the *c* axis within the plane. The sample has the *c*-plane layers with a thin area of 100 nm in thickness and 8 μm in width. A fine magnetic stripe pattern was found along the *c* axis in zero magnetic field

at 5.2 K. The stripe period is about 120 nm. Note that such narrow stripes were inaccessible in the previous magneto-optical studies due to the limited spatial resolution of visible light.[32,33)]

When applying magnetic fields in a direction normal to the film plane, the narrow stripes transformed into the uniformly magnetized state at 80 Oe. The strength of this threshold field is almost similar to that of J'(~126 Oe). With increasing temperature, the stripes did not change in period significantly. They survived even above T_C and eventually disappeared at around 7.3 K. This threshold temperature is in good agreement with the crossover temperature T^* between 2D XY and 2D Heisenberg regimes, which was previously determined by the magnetization and neutron experiments[12)].

The coincidence of the threshold values strongly suggests that the narrow stripes appear as a manifestation of the XY nature of K_2CuF_4. We stress again that the narrow stripes do exist in the 3D and 2D XY regimes and disappear at T^*, above which the XY nature is lost. We may expect that vortices and antivortices are nucleated pairwise by the BKT excitation in the 2D XY regime. However, such a process is not allowed in this sample because of the sample geometry. Instead, the formation of narrow stripe or distorted helical structure indicates that the spins are strongly confined into each layer. In this sense, the stripe formation may be an alternative signature of the XY nature of K_2CuF_4 irrespective of dimensionality (3D or 2D) in real space. Such in-plane confined magnetic structures are compatible with a development of the interlayer correlation with reducing temperature toward T_C through the 2D XY regime, which was previously clarified by the neutron experiments.[12)] Even in the 2D regime, there still remains very weak interlayer correlations which may lead to a stripe formation. The presence of the narrow stripes below T^* seems to be consistent with the picture of the 1D-like solitons of macroscopic spins within the layer discussed in the literature.[31)] As for the formation of magnetic helical structure, an antisymmetric exchange interaction,[42,43)] frequently realized in noncentrosymmetric crystals,[44)] or frustration of exchange interactions among neighboring spins[45)] is required for the formation of chiral helimagnetic order[39)] and symmetric (Yoshimori-type) helix,[46)] respectively. However, such requirements are not likely to be satisfied in K_2CuF_4 crystals. K_2CuF_4 has a centrosymmetric crystal structure and a competition between the first and second neighboring exchange interactions was not reported so far. The origin of the narrow stripes in K_2CuF_4 remains an issue for further investigation. Namely, it is worth considering the possible mechanism generating the stripe pattern in the XY system.

The TEM observations of the narrow stripes with the ac-plane sample should be interpreted as a sign of the presence of 3D and 2D XY regimes in a temperature range below T^* in K_2CuF_4. Next, keeping this feature in mind, the magnetic structures are microscopically examined with varying temperature in the c-plane sample, which is potentially large enough to accommodate vortex and antivortex pairs.

Figure 2 shows Lorentz images of the c-plane sample at temperatures around T_C. Here, a magnetic field of 25 Oe was applied in a direction nearly perpendicular to the plane. However, due to the hard-axis magnetic anisotropy, magnetic moments predominantly lie along the plane. This experimental setup is a favorable one for performing Lorentz microscopy,

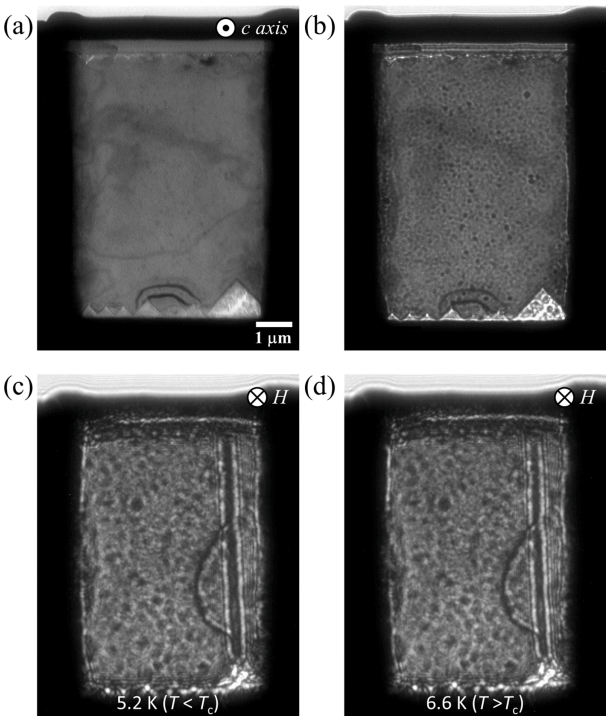

Fig. 2. Lorentz images of the c-plane sample of K_2CuF_4. (a) Infocused TEM image at 5.0 K. The transparent area is 7 μm × 5 μm with the c axis normal to the plane, while its thickness is approximately 0.15 μm, thin enough for the sample to be electron transparent. (b) An underfocused image with ten micrometers defocus at 5.0 K, where many non-magnetic spots were observed. (c and d) Underfocused images with tens of millimeters defocus at 5.2 K and 6.6 K, respectively. A magnetic field of 25 Oe was applied perpendicular to the plane in order to enhance the magnetic contrast. The crack was made in the longitudinal direction on the right side during temperature cycling.

which is sensitive to the magnetic moments normal to the propagation direction of electron beam. We confirmed that applying such a tiny magnetic field caused no significant difference in the formation of magnetic vortices (described below) and was useful for enhancing the magnetic contrast in Lorentz images. Note that the c-plane sample of 150 nm (118 layers) in thickness may contain the stripe pattern. One possible explanation of the stripe pattern is a helical rotation oriented along the c axis with one pitch of the stripe (120 nm) or more at zero magnetic field. In this case, the projected magnetic moments were almost averaged out and thus no contrast was induced by the stripe pattern in Lorentz micrographs. Additional deformation of the magnetic structure from the stripe pattern can be detected via Lorentz microscopy while varying temperature.

Figure 2(a) shows the image in focus, whilst Fig. 2(b) is taken with a defocus of 10 μm. Strong dot contrast was observed to be associated with small pieces of debris on the film. Such debris were found not to exhibit any change in contrast with varying magnetic field or temperature (e.g., even at room temperature), confirming that they were not magnetic in origin. A separate TEM analysis revealed that these debris or precipitates were a few nanometers in diameter. Whilst their origin is unclear, they served as markers to detect position changes as a function of temperature during the temperature variation.

What is clear from Fig. 2(b) is that there is no apparent

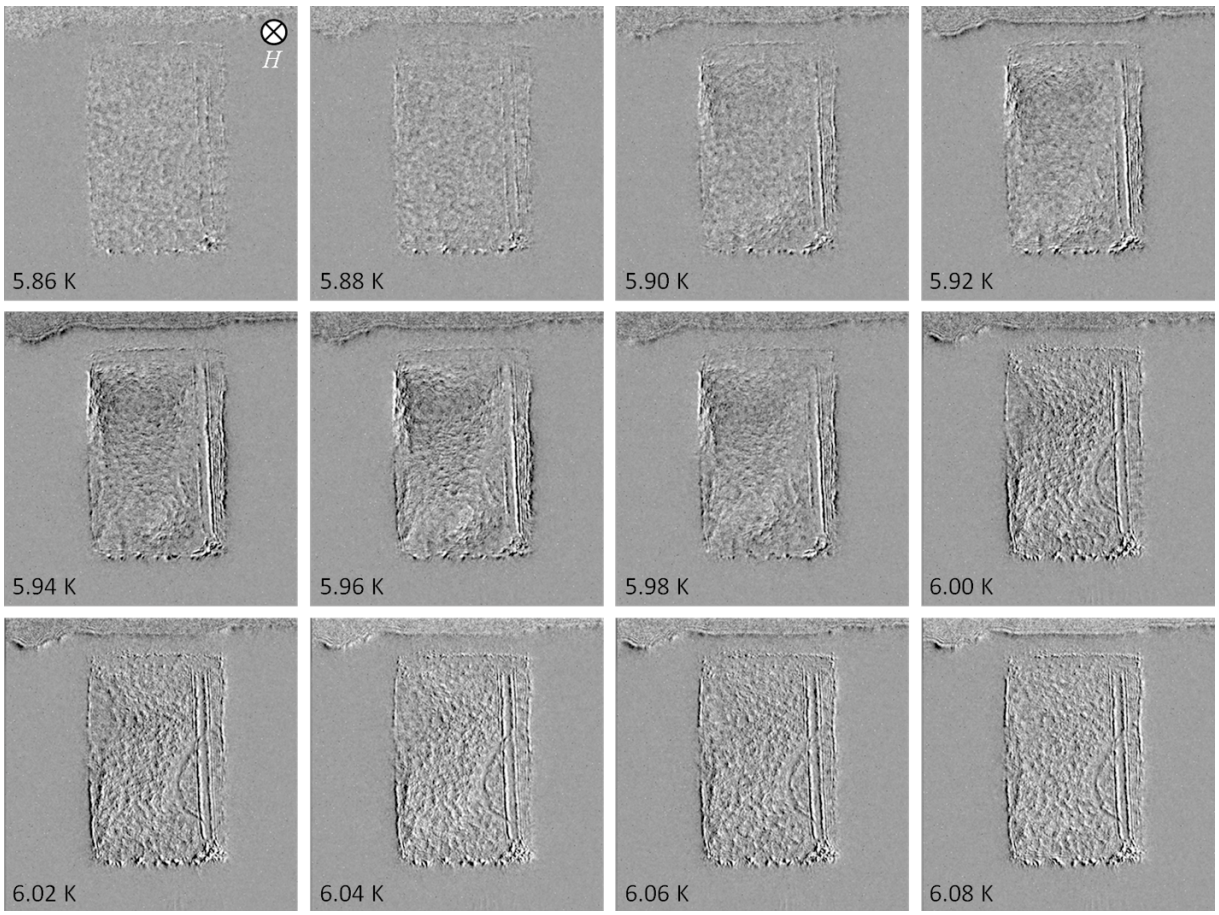

Fig. 3. A series of differential Fresnel TEM images at temperatures from 5.86 K to 6.08 K, made from the underfocused Lorentz images.

magnetic contrast seen at 5.0 K for this imaging condition. One reason could be that, if there were any magnetic structure, the contrast would be subtle with very small changes below T_C. To check this possibility, Lorentz images were taken with a much larger defocus value of tens of millimeters. Two such images at temperatures of 5.2 and 6.6 K are shown in Figs. 2(c) and 2(d), respectively. Whilst there are no clear domain walls, some image distortions between the two images are seen: the left-side edge is expanded in a barrel shape and the slit line on the right side is wider in Fig. 2(c) compared to Fig. 2(d). These observations do indicate that there are detectable effects of the magnetic moment configuration below T_C in the images.

For more clarity, a series of differential Lorentz images from 5.86 K to 6.08 K are shown in Fig. 3, where the disappearance of vortices occurred at around 6 K as described below. The original Lorentz images were taken while the temperature increased from 5.4 K to 8.3 K in a perpendicular magnetic field of 25 Oe. The contrast patterns were observed only in the differential Lorentz images from 5.9 K to 6.0 K, namely in the 3D *XY* regime, while no contrast change was found in temperatures above T_C in the 2D *XY* regime. Contrast changes in the differential image are indicative of the magnetic structure, while the contrast sign depends on a rotation sense of the vortex. An anticlockwise vortex will deflect electrons towards the center, causing a localized brightening. The dark contrast in the upper portion of the sample in the *differential* image indicates that this brightening effect is decreasing as the sample is heated and the magnetic moment reduces. Thus, we can infer the presence of an anticlockwise vortex at the top of the sample and, from the opposite contrast, a clockwise vortex in the bottom section of the sample. Any apparent motion of these vortices were not detected at lower temperatures and they disappeared from view around 6 K with increasing temperature toward T_C. Their appearance and disappearance were reversible with regards to temperature irrespective of the temperature sweep directions.

Magnetic structures were quantified by analyzing distortions of the Lorentz images. First, the image distortions were evaluated by using precipitates as markers. Figures 4(a) and 4(b) show the distortions maps given by arrows as well as in a mesh grid, respectively. Then, such distortions were converted into a color code for a clear visualization of magnetic vortices as shown in Fig. 4(c). We note that the arrows represent the relative integrated induction strength and direction.

Now, we can identify vortex and antivortex structures that possess positive and negative vorticity around the core respectively. Figure 4(d) shows the positions of vortex centers which are inferred from singularity points found in Fig. 4(c). Two vortices exhibit a circular distribution of magnetic moments with a positive unity of vorticity in the upper (#1) and bottom (#3) sections. In addition, one antivortex with a negative vorticity is recognized at the center-left side of the view (#2). The other antivortex is partially found at the sample edge on the center right of the view (#4), while its remaining part may deform along the crack. The vortex and antivortex are likely to

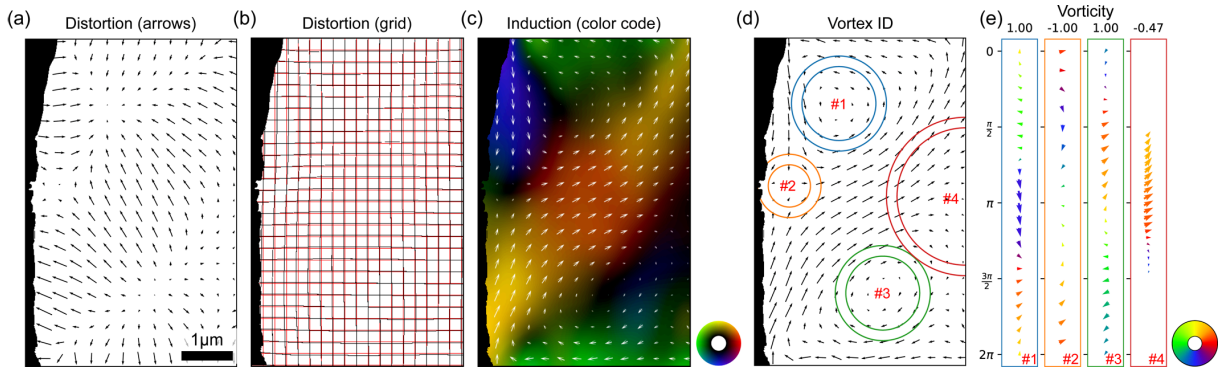

Fig. 4. Arrows (a), mesh grid (b), and color code (c) presentations of the distortions of the Lorentz image shown in Fig. 2(c), processed with BUnwarpJ[47] and the fpd library.[48] Magnetic vortices are clearly visualized in (c). The field of view is set by the sample extent in the top and bottom, and by the crack on the right-hand side. The masked region on the left is where the sample is opaque due to increased thickness. (d) Regions surrounding a 'singularity' where either complete or partial (anti)vortices are identified. (e) A radial profile of a rotation of magnetic induction for each region with the vorticity value at the top. The location correspondence is indicated by number and color in (d) an (e).

be loosely connected and form a pair in both cases (#1,#2 and #3,#4). Namely, it is likely that vortex and antivortex pairs are confined or located in this small area of the *c*-plane sample.

The effect of the finite size sample can be seen in the flux closure pattern that forms. Such patterns are frequently found in a patterned thin film of ferromagnetic materials (i.e., 3D Heisenberg system) because of the demagnetization effect. However, we stress that antivortices of the sort we observe are not usually present, except as a metastable state, indicating that a nontrivial mechanism plays a role in stabilizing the presence of vortex and antivortex pairs in this sample. Further experiments in TEM samples with a much larger area may be useful for reducing the influence of magnetostatic fields on the magnetic structures around the sample edges and clarifying the nature of observed vortices.

Similar Lorentz TEM observations were performed by changing the strength of perpendicular magnetic fields. The vortices and antivortices were observed from zero magnetic field to 50 Oe, while the sample became uniformly magnetized within the plane at larger magnetic fields. These magnetic structures composed primarily of in-plane magnetic components are consistent with the enhanced *XY* character of K_2CuF_4 in this temperature range.[12]

A 3D magnetic structure is inferred from the Lorentz images of vortices. Whilst a vortex pancake could be generated in each layer of K_2CuF_4, its columnar stack is eventually formed via weak interlayer coupling in the confined geometry of the *c*-plane sample. This picture is likely to be consistent with the behavior expected in the 3D *XY* regime. Based on a quantitative evaluation of the magnitude of magnetic induction, it takes about a half value compared to the expected one. Such a reduction of the magnetic induction may be caused by incomplete stacking or close packing of pancakes over half of 120 layers of the *c* plane in thickness. Alternatively, pancakes may fluctuate within the plane to reduce the net induction. Surface damaged layers as artifacts also contribute to reducing the magnetic induction. These features are consistent with the experimental difficulty in detecting vortices by means of the standard Fresnel mode of Lorentz microscopy in this study. Indeed, the vortices we observe in K_2CuF_4 exhibit only weak contrast variations across their core. This contrasts with the case of conventional soft ferromagnetic materials such as permalloy, where the Lorentz micrograph of the magnetic vortex shows sharp contrast at its core.

Perspective. — All the experimental results obtained by cryogenic Lorentz microscopy are summarized in Table I(c). Such microscopic behavior can be compared with magnetic characteristics previously revealed by magnetization and neutron scattering experiments[12] as well as the formation of magnetic vortex and antivortex pairs expected for the BKT phase transition.

Let us first mention briefly theoretical viewpoints. Possible crossover and critical phenomena are governed by three key parameters: J, J', and J_A. The ratio J'/J controls dimensionality of the exchange interaction network, while J_A/J controls anisotropy in the spin space. In the case of the present compound, the values $J'/J \simeq 10^{-3}$ and $J_A/J \simeq 10^{-2}$, leading to a picture of two-step dimensional crossover of the spin system as shown in Table I. Furthermore, the ferromagnetic phase transition associated with broken continuous symmetry is prevented at a finite temperature. Consequently, we expect only the BKT transition is allowed. In this sense, the meaning of $T_C \simeq 6.25$ K should be regarded as a crossover temperature below which ferromagnetic correlations softly evolve. This situation justifies that the BKT transition can survive just below T_C. This view is theoretically pointed out in Ref. [30]. Namely, Hikami and Tsuneto[30] demonstrated the existence of a temperature region below T_C where the two-dimensional scaling still works. In this study, we avoid going further into the exact determination of T_{KT}. Clarification of the relationship between T_C and T_{KT} will be left to future studies.

In this study, the presence of the 2D and 3D *XY* regimes was confirmed microscopically by observing the formation of characteristic magnetic structures at the corresponding threshold temperatures. The remaining issue is whether or not unbound vortices and antivortices exist in the 2D *XY* regime. We do not have a conclusive answer at the moment. Although vortices were observed in the 3D *XY* regime, the vortices may or may not be confined, but our observations certainly were limited in the small area of the sample. This observation suggests that a much larger system of K_2CuF_4 will be advantageous for inducing vortex-antivortex excitations, although large area samples may be challenging to produce. Real-space observation methods of Lorentz microscopy are not good at sensing

vortices in motion because of the lack of temporal resolution. Small-angle electron scattering experiments[49] may be useful for detecting the presence of such moving vortices.

If the experiment were performed in a large bulk K_2CuF_4 sample, magnetic vortices and narrow stripes might coexist in the 2D *XY* regime, as shown in Table I(d). The interlayer correlation develops among the layers with reducing temperature. However, its lengthscale would be limited by the stripe period at a maximum. This picture is likely to hold on a magnetic column of vortices and antivortices. Naively speaking, vortex or antivortex tubes with a finite length along the *c* axis would float and wander around in the stripe background. Then, vortex and antivortex tubes would form a pair at low temperatures below $T_{\rm KT}$. In this respect, we might observe phenomena related to the BKT transition which provide an influence on the magnetic responses in the 2D *XY* and 3D *XY* regimes, though the process of the BKT transition was modified by the interlayer and dipolar interactions.

Concluding remarks. — Our observations of narrow stripes in the 2D *XY* regime as well as vortex-antivortex pairs below $T_{\rm C}$ reveal how the nature of the 2D *XY* spin system is incorporated into 3D magnetic structures in a K_2CuF_4 film with a finite area and thickness. The narrow stripes are likely to be formed as a sign of the *XY* nature below the crossover temperature T^* with developing the interlayer correlation at lower temperatures in the 2D *XY* regime. The vortex-antivortex formation is a possible signature of the BKT transition modified by the interlayer and dipolar interactions.

Finally, we point out that there are some remaining issues; in particular, the origin of the magnetic structures observed in the 2D and 3D *XY* regimes including a possible symptom of the BKT transition. We need to keep in mind that the vortex might be a characteristic pattern of the *XY* system which causes the BKT transition only in the pure 2D case. For clarifying the issue experimentally, a film growth of K_2CuF_4 with atomic-scale thickness will be worth studying in detail to compare against thicker films and to extract the critical exponents that characterize the transition. A development of the interlayer correlation should be hampered in such a very thin film, which leads to retaining the 2D *XY* character and making the BKT excitations robust over a wide range of temperatures. Based on the experimental observations, the targeted value for film thickness can reach about a quarter or half of the stripe period, within which the spins are supposed to orient in the same direction and behave as 2D *XY* spins. The criterion value is not so severe, ranging from 30 nm (24 units) to 60 nm (48 units). This means that the top-down fabrication techniques are still useful for obtaining films with such thicknesses. Note that the required thickness is as large as or smaller than $a\sqrt{J/J'}$ (36 units), which is also a measure of $T_{\rm C}$. Namely, thin films satisfying this criterion will largely suppress the ferromagnetic phase transition and generate the BKT excitations robustly. That the behavior is expected for very thin films is also summarized in Table I(d).

This approach corresponds to the material design strategy of expanding the 2D *XY* regime and generating the robust BKT excitations by impeding the development of the interlayer correlation length. Another possible way is to make J' zero in the material so as to erase the 3D *XY* regime ($T_{\rm C}$) and realize the ideal 2D *XY* system, as presented in Table I(b). As the latter approach involves modification of crystal properties, it is likely to be a very challenging one to achieve.

The BKT phase transition has been sought for in magnetic systems over many decades and still remains largely a mystery. We believe that our study makes an important contribution to understanding the physics behind phase transitions in 2D ferromagnetic materials and realizing the BKT transition in a magnetic system.

Acknowledgement.— We sincerely express our gratitude to Kinshiro Hirakawa for providing us K_2CuF_4 crystals and having fruitful discussions. We also thank Y. Kato, K. Hukushima, G. M. Macauley, J. Ohe, M. Mito, and A. S. Ovchinnikov for useful discussions and a critical reading of the manuscript. We acknowledge support from Grants-in-Aid for Scientific Research (Nos. 17H02767, 17H02923). This work includes the results obtained by using the research equipment shared in the MEXT Project for promoting public utilization of advanced research infrastructure（Program for supporting introduction of the new sharing system: Grant Number JPMXS0410500020) and the United Kingdom research council EPSRC (grant number EP/M024423/1).

1) J. M. Kosterlitz and D. J. Thouless, Long range order and metastability in two dimensional solids and superfluids. (Application of dislocation theory), J. Phys. C: Solid State Phys. **5**, L124-L126 (1972).
2) J. M. Kosterlitz and D. J. Thouless, Ordering metastability and phase transitions in two-dimensional systems, J. Phys. C: Solid State Phys. **6**, 1181-1203 (1973).
3) J. M. Kosterlitz, The critical properties of the two-dimensional xy model, J. Phys. C: Solid State Phys. **7**, 1046-1060 (1974).
4) The Royal Swedish Academy of Science 2016a, Press Release: The Nobel Prize in Physics 2016.
5) H. E. Stanley and T. A. Kaplan, Possibility of a phase transition for the two-dimensional Heisenberg model, Phys. Rev. Lett. **17**, 913-915 (1966).
6) N. D. Mermin and H. Wagner, Absence of ferromagnetism or antiferromagnetism in one- or two-dimensional isotropic Heisenberg models, Phys. Rev. Lett. **17**, 1133-1136 (1966): Erratum Phys. Rev. Lett. **17**, 1307 (1966).
7) V. L. Berezinskii, Destruction of long-range order in one-dimensional and two-dimensional systems having a continuous symmetry group I. Classical systems, Sov. Phys. JETP **32**, 493-500 (1971).
8) V. L. Berezinskii, Destruction of long-range order in one-dimensional and two-dimensional systems having a continuous symmetry group II. Quantum systems, Sov. Phys. JETP **34**, 610-616 (1972).
9) J. M. Kosterlitz and D. J. Thouless, Chapter 1: Early Work on Defect Driven Phase Transitions, in 40 Years Of Berezinskii-Kosterlitz-Thouless Theory, Jorge V Jose, Ed. (World Scientific, Singapore).
10) D. J. Bishop and J. D. Reppy, Study of the superfluid transition in two dimensional ^{4}He films, Phys. Rev. Lett. **40**, 1727-1730 (1978).
11) H. S. J. van der Zant, M. N. Webster, J. Romijn, and J. E. Mooij, Vortices in two-dimensional superconducting weakly coupled wire networks, Phys. Rev. B **50**, 340-350 (1994).
12) K. Hirakawa, Kosterlitz-Thouless transition in two dimensional planar ferromagnet K_2CuF_4 (invited), J. Appl. Phys. **53**, 1893-1898 (1982).
13) I. Yamada, Magnetic properties of K_2CuF_4 –A transparent two-dimensional ferromagnet–, J. Phys. Soc. Jpn. **33**, 979-988 (1972).
14) S. Funahashi, F. Moussa, and M. Steiner, Experimental determination of the spin-wave spectrum of the two-dimensional ferromagnet K_2CuF_4, Solid State Comm. **18**, 433-435 (1976).
15) H. Yamazaki, Parallel pumping of the Brillouin-zone-boundary magnons in a two-dimensional ferromagnet K_2CuF_4, J. Phys. Soc. Jpn. **37**, 667-672 (1974).
16) A. S. Borovik-Romanov, N. M. Kreines, V. G. Zhotikov, R. Laiho, and T. Levola, Optical detection of ferromagnetic resonance in K_2CuF_4, J. Phys. C: Solid State Phys. **13**, 879-885 (1980).
17) S. B. Khokhlachev, Two-dimensional Heisenberg model with weak

anisotropy, Sov. Phys. JETP **43**, 137-141 (1976).
18) A. Z. Patashinsky and V. I. Pokrovsky, Fluctuation theory of phase transitions (Pergamon, Oxford, 1979).
19) K. Hirakawa and H. Yoshizawa, Observation of the condensation of magnons in the quasi-two-dimensional planar ferromagnet K_2CuF_4, J. Phys. Soc. Jpn. **47**, 368-378 (1979).
20) K. Hirakawa, G. Shirane, and J. D. Axe, Reexamination of anomalous magnetic intensity in 2D ferromagnet K_2CuF_4, J. Phys. Soc. Jpn. **50**, 787-791 (1981).
21) K. Hirakawa, H. Yoshizawa, and K. Ubukoshi, Neutron scattering study of the phase transition in two-dimensional planar ferromagnet K_2CuF_4, J. Phys. Soc. Jpn. **51**, 2151-2158 (1982).
22) K. Hirakawa, H. Yoshizawa, J. D. Axe, and G. Shirane, Neutron scattering study of spin dynamics at the magnetic phase transition in two-dimensional planar ferromagnet K_2CuF_4, J. Phys. Soc. Jpn. **52**, 4220-4230 (1983).
23) K. Hirakawa and H. Ikeda, Neutron scattering experiments on the two-dimensional ferromagnet K_2CuF_4, J. Phys. Soc. Jpn. **33**, 1483 (1972).
24) K. Hirakawa and H. Ikeda, Investigations of two-dimensional ferromagnet K_2CuF_4 by neutron scattering, J. Phys. Soc. Jpn. **35**, 1328-1336 (1973).
25) H. Kubo, K. Shimohigashi, I. Yamada, Magnetization of two-dimensional ferromagnet K_2CuF_4, J. Phys. Soc. Jpn. **34**, 1687 (1973).
26) H. Kubo, Magnetization of the two-dimensional Heisenberg ferromagnet K_2CuF_4 with small XY-like anisotropy, J. Phys. Soc. Jpn. **36**, 675-684 (1974).
27) A. Dupas and J.-P. Renard, Comportement critique de ferromagnétiques proches du modèle de Heisenberg a deux dimensions, J. Phys. (Paris), Colloq. **37**, C1-213-C1-217 (1976).
28) K. Hirakawa and K. Ubukoshi, Magnetization measurements of two-dimensional planar ferromagnet K_2CuF_4, J. Phys. Soc. Jpn. **50**, 1909-1916 (1981).
29) S. Miyashita, H. Nishimori, A. Kuroda, and M. Suzuki, Monte Carlo simulation and static and dynamic critical behavior of the plane rotator model, Prog. Theor. Phys. **60**, 1669-1685 (1978).
30) S. Hikami and T. Tsuneto, Phase transition of quasi-two dimensional planar system, Prog. Theor. Phys. **63**, 387-401 (1980).
31) K. Hirakawa and H. Yoshizawa, Kotaibutsuri **14**, 747-757 (1979).
32) W. Kleeman and F. J. Schäfer, Magneto-optical studies on ferromagnetic stripe domains in K_2CuF_4, J. Magn. Magn. Mater. **21**, 143-156 (1980).
33) W. Kleemann and J. Ferré, Bragg-regime diffraction and waveguiding of light by ferromagnetic domains in K_2CuF_4, Phys. Rev. B **24**, 1568-1571 (1981).
34) T. Kawasaki, T. Yoshida, T. Matsuda, N. Osakabe, A. Tonomura, I. Matsui, and K. Kitazawa, Fine crystal lattice fringes observed using a transmission electron microscope with 1 MeV coherent electron waves, Appl. Phys. Lett., **76**, 1342-1344 (2000).
35) A. Tonomura, H. Kasai, O. Kamimura, T. Matsuda, K. Harada, Y. Nakayama, J. Shimoyama, K. Kishio, T. Hanaguri, K. Kitazawa, M. Sasase, and S. Okayasu, Observation of individual vortices trapped along columnar defects in high-temperature superconductors, Nature **412**, 620-622 (2001).
36) K. Harada, J. Endo, N. Osakabe, and A. Tonomura, Direction-free magnetic field application system, e-J. Surf. Sci. Nanotech., **6**, 29-34 (2008).
37) Y. Togawa, K. Harada, T. Akashi, H. Kasai, T. Matsuda, F. Nori, A. Maeda, and A. Tonomura, Direct Observation of Rectified Motion of Vortices in a Niobium Superconductor, Phys. Rev. Lett. **95**, 087002 (2005).
38) A. Tonomura, Electron holography, 2nd edn. (Springer, Heidelberg, Germany).
39) Y. Togawa, T. Koyama, K. Takayanagi, S. Mori, Y. Kousaka, J. Akimitsu, S. Nishihara, K. Inoue, A. S. Ovchinnikov, and J. Kishine, Chiral magnetic soliton lattice on a chiral helimagnet, Phys. Rev. Lett. **108**, 107202 (2012).
40) R. H. Wade, The measurement of magnetic microfields, IEEE Trans. Magn. **12**, 34-39 (1976).
41) H. Suzuki, T. Shimakura, K. Itoh, and K. Nakamura, Magnetic head field over the air-bearing surface as visualized by the projection of a patterned electron beam, IEEE Trans. Magn. **36**, 3614-3617 (2000).
42) I. E. Dzyaloshinskii, A thermodynamic theory of weak ferromagnetism of antiferromagnetics, J. Phys. Chem. Solids **4**, 241 (1958).
43) T. Moriya, Anisotropic superexchange interaction and weak ferromagnetism, Phys. Rev. **120**, 91 (1960).
44) Y. Togawa, Y. Kousaka, K. Inoue, and J. Kishine, Symmetry, structure, and dynamics of monoaxial chiral magnets, J. Phys. Soc. Jpn. **85**, 112001 (2016).
45) A. Yoshimori, J. Phys. Soc. Jpn. **14**, 807 (1959).
46) T. Koyama, S. Yano, Y. Togawa, Y. Kousaka, S. Mori, K. Inoue, J. Kishine, and J. Akimitsu, Unconventional Magnetic Domain Structure in the Ferromagnetic Phase of MnP Single Crystals, J. Phys. Soc. Jpn. **81**, 043701 (2012).
47) I. Arganda-Carreras, C. O. S. Sorzano, R. Marabini, J.-M. Carazo, C. Ortiz-de Solorzano, and J. Kybic, Consistent and Elastic Registration of Histological Sections using Vector-Spline Regularization, in Lecture Notes in Computer Science, R. R. Beichel and M. Sonka, Ed. (Springer, Berlin Heidelberg).
48) FPD: Fast pixelated detector data storage, analysis and visualisation, available at `https://gitlab.com/fpdpy/fpd`, accessed 8 March 2020.
49) Y. Togawa, Small-angle electron scattering of magnetic fine structures, Microscopy **62**, S75 (2013).